*Semiconductor Physics, Quantum Electronics & Optoelectronics, 2012. V. 15, N 3. P. 239-246.*

PACS 61.72.Cc, 66.30.Lw, 78.55.Et

# The factors influencing luminescent properties of ZnS:Mn obtained by the method of one-stage synthesis

**Yu.Yu. Bacherikov[1], A.G. Zhuk[1], S.V. Optasyuk[1], O.B. Okhrimenko[1], K.D. Kardashov[2], S.V. Kozitskiy[3]**
[1]*V. Lashkaryov Institute of Semiconductor Physics, NAS of Ukraine,*
*41, prospect Nauky, 03650 Kyiv, Ukraine; e-mail: Yuyu@isp.kiev.ua*
[2]*O. Popov Odessa National Academy of Telecommunications*
*1, Kuznechnaya str., 65029 Odessa, Ukraine*
[3]*Odessa National Maritime Academy*
*8, Didrikhson str., 65029 Odessa, Ukraine*

**Abstract.** Considered in this paper is the model that combines appearance of defects responsible for self-activated (SA) emission in ZnS with its piezoelectric properties. Being based on analysis of the luminescence spectrum, the authors demonstrate the influence of mechanical destruction, impact of ultrasound, microwave radiation and pulsed magnetic field on the emission efficiency for centers of luminescence connected with intrinsic defects in ZnS:Mn prepared using the method of self-propagating high-temperature synthesis (SHS). It has been shown that downsizing the ZnS:Mn crystals prepared according to the above method as well as more discrete differentiation of phases present in this material due to development and growth of inner boundaries and surface under external actions leads to quenched SA-photoluminescence with $\lambda \sim 400–525$ nm.

**Keywords:** self-activated luminescence, ZnS:Mn, mechanical destruction, ultrasonic action, super-high-frequency radiation, pulsed magnetic field.

Manuscript received 18.06.12; revised version received 15.08.12; accepted for publication 10.09.12; published online 25.09.12.

## 1. Introduction

Recently, the possibilities of self-propagating high-temperature synthesis (SHS) for obtaining luminophoric materials based on zinc sulphide [1, 2] have been studied ever more actively. Transfer from traditional furnace technologies to SHS has practically changed the approaches to the formation of solid-state materials in the course of their obtaining and post-technological processing. Technological possibilities of SHS are very wide, in particular, they allow to realize material doping by using various elements and compounds during the synthesis. A variety of organizational methods of the burning process in the SHS wave provides a possibility to obtain a desired product either in the form of a cast sample with the sizes being given, or in the form of powder with necessary dispersion, including nano-powders with the most required sizes close to 1–5 nm.

However, for the maximum application of the new possibilities discovered in the process of SHS, needed is more thorough investigation of the processes involved in the synthesis and the subsiquent post-technological processing of the obtained materials. The obtained material structural peculiarities, which can be revealed in different forms depending on the conditions of the synthesis, should be taken into consideration as well. As for ZnS, a number of authors [3-5] explain the difficulties in preparation of *p*-type ZnS and the oxygen-free one by thermodynamic and crystal-chemical properties of its structure. Meanwhile, in the works dealing with luminophor ZnS, it is not considered as a piezoelectric [3-5, 6], and in the works dealing with piezoelectric effect of ZnS it is not regarded as a luminophor [7].

So, to ground the formulation of the task of this paper, we will consider the factors influencing the formation of structural peculiarities of the powdery ZnS in the course of its synthesis, taking into account its piezoelectric properties.

## 2. The causes of the emergence of intrinsic defects in ZnS in the course of its SHS

Analyzing the formation of ZnS lattice structure, which is influenced by both external factors and internal processes, we will take into account synthesis conditions of material, as well as structural peculiarities of ZnS itself. It should be noted that SHS is a physical-chemical

process running in an extreme mode at the expense of internal energy resources of the reacting substances, and it is characterized by high temperature of the process, high rate of the burning front propagation, and maximum heating the substance in the burning wave [8]. All these factors lead to fast pressure and temperature changes in the reaction zone. Since, during the synthasis, the lattice structure of material is formed with regard to the maximum free energy $G$ of the obtained crystal, there arise several such minima in a wide range of temperatures and pressures, and for each of them there is a separate corresponding lattice structure with its typical character of bonds. It is shown in this paper that at physical-chemical analysis of ultradisperse systems it is necessary to take into consideration a dispersion degree of substance. On the basis of this approach, it is explained in [9] interrelation between the dispersion degree of material and temperature, which causes fusion, polymorphic transmutations and sintering; and the influence of dispersion on the diffusion constant in separate crystal grains and on chemical activity of the obtained substance. The authors [9] assert that regardless of the method of producing a disperse system, its redundant energy is defined either by surface energy, or by formation of metastable solutions.

Another aspect that should be taken into account when analyzing the processes influencing the structure of ZnS at the growth of its crystals is piezoelectric properties of ZnS. ZnS is ionic crystal, and, as a result of non-coincidence of its catonic and anionic centres, it has the electrical moment. According to [7], piezoelectric modulus of ZnS (Coul/m$^2$): $e_{15} = -0.118$, $e_{31} = -0.238$, $e_{33} = 0.265$. As it is known, the piezoelectric effect can exist only in those crystals, which unit cells have no centres of symmetry [10]. In these crystals, polarization caused by the electrical moment in the absence of free charge carriers (for example, in quartz) leads to the displacement of ions from their lattice stices, which is responsible for appearance of a polarization charge, to such a position, at which this charge disappears. It is, actually, equivalent to occurrence of electrically induced strain. In a crystal that has free charge carriers (for example, in ZnS), polarization is partially compensated by localization of free charge carriers on the surface, and in real crystals even at inner boundaries and other structural defects, and only then it leads to strains. That is why, when achieving a certain value of the polarization vector and under deficit of free carriers, it becomes more profitable for a crystallite, from the energy viewpoint, to form boundaries and various intrinsic defects. Appearance of boundaries, consequently, leads to formation of a group of crystallites. Then, within frames of separate crystallite polarization has a definite value, and within a group of differently oriented crystallites, i.e. in a synthesized material, it is, on the average, equal to zero [11]. Here it is necessary to clarify that increasing the total electrical moment of a growing crystallite is related not to the growth of its total dimensions, but only to the growth of the surface areas of those facets that are perpendicular to piezoelectric axes [12]. This is supported by the data [13, 14], which show that when preparing ZnS by a chemical vapor deposition method, a defective and disordered structure is formed, and ZnS itself grows in a nonstoichiometric manner [14] with microstresses of II kind [13]. Microstresses of II kind show that the system of atomic planes in the material, instead of strictly defined interplanar spacing ($a$), has interplanar spacings, laying in the limits $a \pm \Delta a$ [15].

At the same time, appearance of intrinsic defects, on the one hand, increases the concentration of free carriers, raising their contribution to compensation of polarization, and, on the other hand, at their structurization there can be formation of separate ZnS unit cells with interstitial zinc ($Zn_i$) in the centre of these cells and $V_{Zn}$ in its nearest surrounding, which compensates the charge of $Zn_i$. Being in this configuration, $Zn_i$ plays a role of the centre of symmetry for the Coulomb potential of this cell with its electrical moment equal to zero. This is supported by a number of works, dealing with self-activated (SA) luminescence in ZnS, caused, according to [3, 4, 16-20], by defects, in particular, $V_{Zn}$ and $Zn_i$ at their either separate, or simultaneous formation. This unsteady state (close and simultaneous existence of $V_{Zn}$ and $Zn_i$) can tranfer into a metastable state only under certain conditions.

As it was said above, in the course of synthesis, the crystalline structure of material is formed, taking into account a minimum of free energy $G$. In case of SHS, the free energy $G$ of the system consisting of a crystal (a condensed phase with free energy $G_1$) and an environment (vapor phase of reagents with free energy $G_2$) can be presented in the form:

$$G = G_1 + G_2 + \sigma A, \qquad (1)$$

where $\sigma$ is the specific free surface energy coinciding in this case with the surface tension one, $A$ – interphase surface area [21, 22]. In the case of ZnS synthesis, as well as similar piezoelectrics, it is necessary to take into account contribution of two more components to a free energy: the contribution of the energy provided by electrical polarization $G_{EP}$, and $G_e$ – free energy of charge carriers. The latter component $G_e$ characterizes the part of a free energy related, in particular, to a recharge of particles (atoms, molecules), which accompanies the process of synthesis [23]. So:

$$G = G_1 + G_2 + \sigma A + G_{EP} + G_e. \qquad (2)$$

Reducing the sizes of a single piezocrystallite provides contribution increase of $\sigma A$, as well as contribution decrease of $G_{EP}$ into the crystal free energy. Though, it is necessary to take into consideration, as well that the total contribution $\sum_i G_{EP}^i$ of a group of crystallites $i$ with a regular geometrical shape turns to be higher, as compared with that of a single crystal $G_{EP}^K$, consisting of the same material quantity.

In the single crystal, at the growth of its facets, which are perpendicular to piezoelectric axes, the potential conditioned by localization of charge carriers, compensating polarization, having reached a definite value, is able to cause a serious rearrangement of srtuctural elements in the material and changes in some of its properties in the surrounding area, which leads to the increase of $G$ within the whole system. In this situation, the probability of structuring the intrinsic defects into a configuration with interstitial zinc in the centre of the unit cell of ZnS and $V_{Zn}$ in its closest environment sharply increases. This configuration provides compensation of the electrical moment without participation of free charge carriers, and thus, there is neither their localization on the boundaries, nor formation of boundaries for dicreasing $G$. This will be more advantageous for the system in terms of energy when:

$$G_V + G_i + \Delta G_C + \Delta G_S < \\ < \sum_i \Delta G^i_{EP} + \sum_i \Delta G^i_e + \sum_i \Delta(\sigma^i A^i)\,. \qquad (3)$$

Where $G_V$ is the free energy of vacancies, $G_i$ – free energy of interstitial atoms, $\Delta G_C$ corresponds to the change in the coupling energy contribution, $\Delta G_S$ corresponds to the increase of contribution in $G$ at the violation of the symmetry. Stability of a pair of interstitial zinc in the centre of a unit cell and $V_{Zn}$ in its closest environment will be determined by stability of the electrical potential preventing this pair from annihilation and migration. The change of the potential value in the area of $Zn_i$ and $V_{Zn}$ localization should lead either as a result of moving away of the surface while its growing, or under the influence of external factors, to surface destruction and, consequently, to weakening the SA-luminescence intensity.

Basing on representations of the model mentioned above, which explains the origion of the defects in ZnS:Mn, as those, responsible for SA-luminescence, as well as similar to them, we have formulated the following purpose of the paper: on the basis of luminescent methods of research to find out the influence of mechanical destruction (MD), ultrasonic action, super-high-frequency radiation (SHF-radiation) and the influence of pulsed magnetic field (PMF) on luminescence properties of ZnS:Mn obtained using SHS method.

## 3. Experimental

In this work, we used powders of ZnS:Mn obtained by the method of self-propagating high-temperature synthesis (SHS) [1, 2]. The concentration of Mn impurity in the samples was 1 wt.%. Sulphur and zinc were taken in a stoichiometric relation. Synthesis of the samples proceeded in nitrogen atmosphere. Manganese was entered into material in the form of MnS. The as-synthesized sample represented a conglomerate of ZnS:Mn powder grains, which was formed during the synthesis. The obtained sample was divided into pieces and exposed to the following processings: mechanical destruction, ultrasonic action, radiation and pulsed magnetic field (PMF). MD of ZnS: Mn powder conglomerate was carried out manually in the process of its powdering and grinding in a porcelain mortar. Ultrasonic processing lasted for 20 min in an ultrasonic bath with the frequency 18 kHz, power 250 W, and specific power 0.05 W/cm$^3$. The material was plunged into alcohol. The energy transfered by ultrasonic wave was calculated according to [24] and is equal to $9.9\cdot10^{-4}$ eV. The SHF-radiation processing was carried out for 1 min in the operation chamber with magnetron frequency 2.45 GHz and specific power 0.04 W/cm$^3$. The energy transferred by a single SHF-wave is equal to $9.5\cdot10^{-5}$ eV [25]. The processing by pulsed magnetic field with the amplitude of magnetic field induction ($B_{max}$) equal to 0.3 Tl was carried out in solenoid consisting of 17 coils, with the quantity of pulses equal to 50. The energy obtained by material for one pulse was calculated according to [26] and was equal to 4.8 J/cm$^3$.

Photoluminescence spectra (PS) and luminescence excitation spectra (LES) were obtained using the monochromator SDL-2 at $T$ = 300 K. To excite PS, a nitrogen laser LGI-23 ($\lambda$ = 337 nm) was used. When recording LES, the excitation of the samples was carried out by using xenon lamp radiation, after its passing through the monochromator MDR – 12.

## 4. Experimental results

As seen from Fig. 1a, PS of ZnS:Mn powders, obtained using SHS method, as a result of synthesis, consists of two wide complex bands, which have their maxima in the region $\lambda_{max}$ ~ 455 and 590 nm. The dominating spectral band with $\lambda_{max}$ ~ 590 nm is characteristic of ZnS doped with Mn. This band is complex and consists of a set of single bands with $\lambda_{max}$ equal to 557, 587, 600 nm, conditioned by various localization of Mn impurity atoms in the crystalline lattice of ZnS (Fig. 1b). The band with $\lambda_{max}$ = 600 nm is related to $Mn^{2+}$ ions in octahedral interstitial sites, while the band with $\lambda_{max}$ = 578 nm is related to $Mn^{2+}$ ions close to dislocations or point defects [27]. The majority of authors [27-29] relate the band with $\lambda_{max}$ ~557 nm to the centres formed by the ions of manganese located in the sublattice of zinc in the sites of severe lattice distortion. A number of authors [30] consider the emission band with $\lambda_{max}$ = 557 nm to be complex and conditioned by radiation from several centres located in tetrahedral sites of ZnS crystalline lattice and surrounded by defects.

The second PS band of powder ZnS:Mn, obtained by the SHS method with $\lambda_{max}$ ~ 455 nm, is also complex, and, depending on material stoichiometry, it represents either one wide photoluminescence band (Fig. 1a), or at least two bands with $\lambda_{max}$ ~ 457 nm and 505 nm

(Fig. 1b). According to the literature data, the following bands are characteristic of this region of ZnS photoluminescence spectrum. The band with $\lambda_{max}$ ~ 435 nm is caused by oxygen in ZnS [4], as well as the band with $\lambda_{max}$ ~ 404 nm. The authors [31] relate the band with $\lambda_{max}$ = 405–415 nm, observed in ZnO, to a singly positively charged associator of the type $(V'_{Zn} - V_O)$. According to the authors [32, 33], $\lambda_{max}$ ~ 496 nm is related to the centre – associator ($V_{Zn}Cl_S$), $\lambda_{max}$ ~ 466 nm – to $Zn_i$, and $\lambda_{max}$ ~ 405 nm – to $V_S$. Herein, it is necessary to note that in pure ZnS, in the case of its stoichiometry change, SA-luminescences type of ZnS changes as well: from 445–400 nm at an excess of zinc, to ~365 nm for stoichiometric composition, and 505–510 nm at a sulphur excess, which authors [16, 17] explain by recharge of oxygen complexes participating in SA-luminescence.

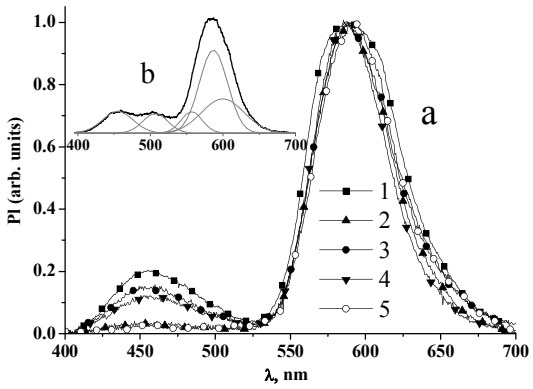


**Fig. 1.** Photoluminescence spectra of ZnS:Mn prepared using the SHS method for: (a) stoichiometric ratio of Zn and S in charge normalized by the maximum of luminescence brightness, *1* – after synthesis and additional processings, *2* – ultrasonic action, *3* – SHF-radiation, *4* – PMF, *5* – mechanical grinding the conglomerates of material; (b) excess of sulphur in charge.

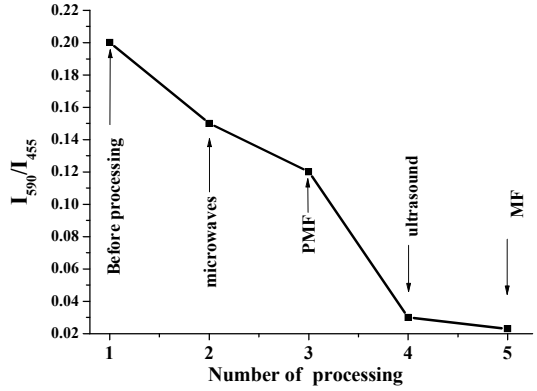


**Fig. 2.** Relationships between intensities of bands with $\lambda_{max}$ ~455 nm and ~590 nm after various processings ZnS:Mn. Abscissa: *1* – before processing, *2* – SHF- radiation, *3* – PMF, *4* – ultrasonic action, *5* – mechanically grinded.

It is necessary to note that destruction of powder conglomerates under the influence of external action (mechanical destruction, ultrasonic action) that can disperse it, results either in a considerable intensity drop of the band with $\lambda_{max}$ ~ 455 nm with respect to the band with $\lambda_{max}$ ~ 590 nm, or in its almost absolute disappearance (Figs 1a and 1b). Besides, despite the fact that this band is superposition of a set of single photoluminescent bands, its shape remains unchanged under the influence of any processing (mechanical destruction, ultrasonic action, super-high-frequency radiation, pulsed magnetic field processing) used by us, i.e. all kinds of the treatments influence equally every single band, which makes up the total band with $\lambda_{max}$ ~ 455 nm. Besides, MD leads to appearance of luminescence in ZnS:Mn in the course of its disintegration, unlike other processings, which action has not provided a visible luminescence. This luminescence at MD can be a manifestation of triboluminescence, electroluminescence and deformation luminescence [34]. However, to provide a more accurate interpretation of luminescence, influenced by mechanical destruction, further studies are needed.

The influence of processings of synthesized ZnS:Mn apart from intensity redistribution between the bands with $\lambda_{max}$ ~ 455 and 590 nm has led to the change of the half-width for the band with $\lambda_{max}$ ~ 590 nm in its photoluminescence spectrum (Fig. 1). As seen from Fig. 1, the band half-width with $\lambda_{max}$ ~ 590 nm changes unsymmetrically under different processings, i.e., the shifts of short-wave and long-wave edges of the band at the half-width level change asynchronously. It indicates that the change of the band half-width is related not only to the change of stress values and concentrations of structural defects in material, but first of all, to intensity redistribution of the single bands, making up a complex band with $\lambda_{max}$ ~ 590 nm (Fig. 1). As seen from Fig. 1a, the greatest intensity drop of the band with $\lambda_{max}$ ~ 600 nm, caused by $Mn^{2+}$ ions in octahedral interstitial sites, relative to the dominating band with $\lambda_{max}$ ~ 578 nm, has occurred as a result of PMF. Other actions also have led to its drop, but not so strong. A short-wave edge shift, i.e. a quenching value of the band ($\lambda_{max}$ ~ 557 nm), conditioned by $Mn^{2+}$ located near dislocations or isolated defects, has appeared to be identical for all processings.

Fig. 3 shows the luminescence spectra corresponding to the peak luminescence ($\lambda_{max}$ ~ 590 nm) of the samples without their recalculation on an instrument function of installation, and normalized by the band of fundamental excitation. As seen from Fig. 3, the luminescence spectra contain five bands with maxima $\lambda_{max}$ ~ 344, 395, 420, 465, 493 nm. The band with $\lambda_{max}$ ~ 344 nm corresponds to the region of fundamental absorption for ZnS. The bands with $\lambda_{max}$ ~ 395, 420, 465, 493 nm correspond to those known from the literature [28, 35] elementary manganese bands of luminescence excitation. These bands are conditioned by

transitions from the basic state $Mn^{2+}$ $^6A_1$ into the excited ones $^4T_1$, $^4T_2$, $^4E_1$, $^4A_1$ [28, 35]. It should be pointed out that the presence of a number of small levels located at the bottom of the conduction band, caused by a considerable quantity of various defects in the material, leads to degradation of a band edge of ZnS, which is well seen (Fig. 3) from a low resolution of the band with $\lambda_{max}$ ~ 395 nm as a single band. It partially concerns, as well, the band with $\lambda_{max}$ ~ 420 nm, which shape is distorted owing to overlapping with tails of other absorption bands. According to [18], in this region, there are bands with $\lambda_{max}$ close to 367 and 395 nm, conditioned by transitions in oxygen aggregations with participation of impurities. The authors of [18, 19] consider that these transitions are $E(\mathrm{Cu(I)}) \rightarrow E_-$ and $E(\mathrm{Cu(I)}) \rightarrow E(\mathrm{Cu}_i)$, respectively. According to [20], the spectral position of the excitation band with $\lambda_{max}$ = 367 nm, as well as the edge of additional absorption corresponding to this band and related to $E_-$, at $\lambda_{max}$ ~ 350 nm determine the concentration of dissolved oxygen in aggregations: ~3 mol.%.

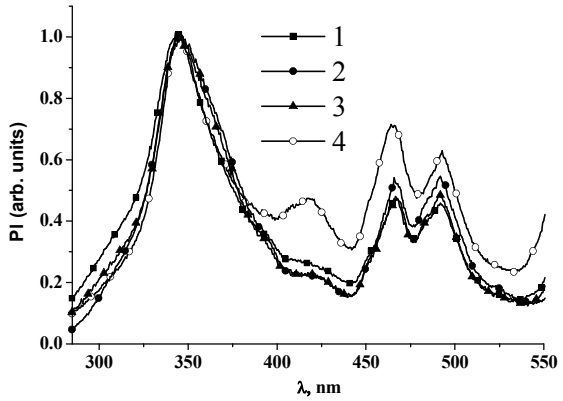


**Fig. 3.** Luminescence excitation bands with $\lambda_{max}$ ~ 590 nm normalized to the peak of band-to-band excitation for ZnS:Mn: *1* – after synthesis and subsequent additional processings, *2* – after ultrasonic action, *3* – SHF-radiation, *4* – PMF.

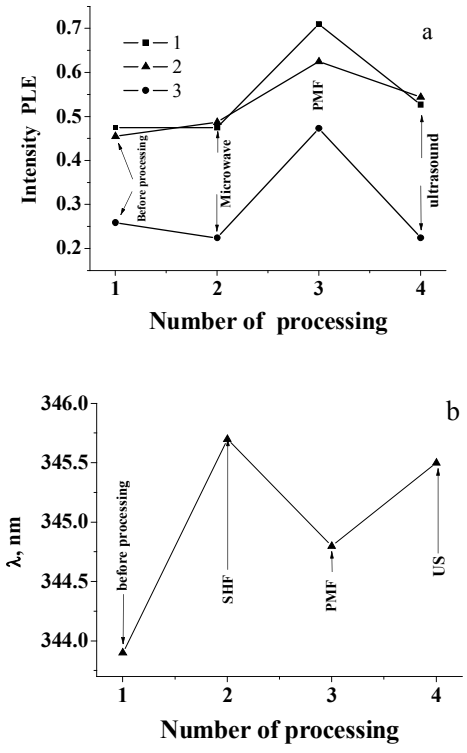


**Fig. 4.** a) Intensity of luminescence excitation bands: $\lambda_{max}$~ 467 (*1*), 495 (*2*), 418 nm (*3*); b) position of the peak for band-to-band excitation after various processings ZnS:Mn. Abscissa: *1* – before processing, *2* – SHF-radiation, *3* – PMF, *4* – ultrasonic action, *5* – mechanically grinded.

The differences between the photoluminescence excitation spectra of ZnS:Mn after various processings are revealed in redistribution of the band intensities (Fig. 4a), as well as in a small shift of the band-to-band region (Fig. 4b). The maximum shift towards the long-wave region of the band for photoluminescence spectra of ZnS:Mn following grinding and ultrasonic action is close to 4 nm relatively to photoluminescence spectra of the basic ZnS:Mn. The shift of the fundamental absorption band suggests the presence of mechanical tensile stresses in the material, which is, evidently, related to a considerable quantity of dislocations and the inner boundaries in it, caused by the synthesis conditions [36].

## 5. Discussion of the results

The most considerable changes in photoluminescence spectra of ZnS:Mn after its various processings have occurred in the group of bands of luminescence in the region $\lambda_{max}$ ~400–525 nm. As it was noted above, according to the literature data [16-19], infact all the centres, responsible for the observed radiation in the region $\lambda_{max}$ ~ 400–525 nm include defects, which also participate in the formation of centres, responsible for SA-luminescence in ZnS. Almost all the authors relate one SA-band or several bands of this group to the complexes including $Zn_i$ and $V_{Zn}$ simultaneously. This neighborhood, instead of transition of interstitial Zn to its own vacancy, turns to be advantageous in terms of energy only with account of all the components, located in the environment of an elementary cell or a set of cells of ZnS. As it has already been shown in the paper, the configuration, at which Zn appears to be the centre of symmetry for the Coulomb potential of this unit cell allows to lower the value of the electrical moment and, hence, to lower the value *G* of the whole ZnS crystallite. Therefore, this configuration proves to be rather stable. The role of interstitial Zn atoms, as fast diffusing intrinsic donors participating in the establishment of equilibrium interaction between its point defects, is proved by the data [20] as well. The authors [20] consider $O_S$ as a centre, the nearest environment of which is reconstructed and which creates a mutually related set of defects.

At SHS of ZnS, in different time intervals of the reaction the material is formed under essentially different thermodynamic conditions. As a result of this, the obtained ZnS, apart from mechanical stresses (in this case tensile stresses), has almost all the defects typical of the most different ZnS modifications, including complexes $\left\{ O_S^* \cdot Zn_i^{\bullet} \cdot V_{Zn}'' \right\}$, formation of which, according to [20], is possible only at interstitial zinc deficiency in a crystal, and donor-acceptor pairs $\left\{ O_S^* \cdot Zn_i^{\bullet} \cdot V_{Zn}'' \right\}' - Zn_I^{\bullet}$, which are formed at an excess of zinc [20]. According to the Gibbs phase rule, of all phases ($k + 2 \geq j$, where $k$ is the number of components of the system), only one of three possible phases is in a stable state for the given thermodynamic conditions, the others are in a metastable state [22]. Thus, under any external action, regardless of its type, i.e., leading either to manifestation of the piezoelectric effect (mechanical destruction, ultrasonic action), or to manifestation of the inverse piezoelectric effect (SHF-radiation, the influence of pulsed magnetic field), relaxation of internal stresses in the material takes place, which is accompanied by layering of the available phases and rearrangement of crystalline and defective structures. This, in its turn, leads to destruction of the complexes responsible for SA-luminescence, which is well seen from Figs. 1 and 2. The destruction of the complexes is, evidently, caused by concentration reduction of the defects within these complexes, as well as spatial separation of the defects.

In polycrystalline materials, owing to the presence of grain boundaries, stress relieve is achieved, as a rule, by relaxing these boundaries, i.e. either as a result of directed displacement of atoms through the boundaries (diffusion plasticity), or as a result of sliding on them [37]. Therefore, we can assume that the defects, responsible for the bands, making up a wide band $\lambda_{max} \sim$ 455 nm (radiation in the region ~400–525 nm) are mainly concentrated in the regions with fuzzy interphase boundaries, localizations of structural defects, etc., i.e. in those places, where there is a possibility with increasing stress to develop inner boundaries or where they are already available. As it is seen from Fig. 2, mechanical destruction and ultrasonic action leads to almost total disappearance of the band with $\lambda_{max} \sim$ 455 nm, unlike SHF-radiation and pulsed magnetic field, which lead only to its attenuation in 1.5–2 times. At the same time, the influence of processings on behavior of the bands caused by Mn participation in recombination of carriers has rather different character. SHF-radiation and ultrasonic action have led to similar intensity changes of the bands with $\lambda_{max} \sim$ 557 and 600 nm, i.e. to an identical shift of short-wave and long-wave edges of the band with $\lambda_{max} \sim$ 590 nm (Fig. 1) and to the intensity change of Mn bands of luminescence excitation spectra as regard to band-to-band absorption (Fig. 4). PMF has led to the maximum, as compared with the other processings, intensity drop of the photoluminescent band with $\lambda_{max} \sim$ 600 nm and to the maximum intensity growth of luminescent Mn bands. This different influence on luminescent and photoluminescent bands under various processings is related, on the one hand, to specificity of each specific action, and, on the other hand, to a different nature of recombination and excitation processes, responsible for photoluminescent and excitation bands.

Similar values of the band quenching with $\lambda_{max} \sim$ 455 nm under the influence of mechanical destruction and ultrasonic action processings are, evidently, related to the same processes proceeding in ZnS:Mn at their interaction. Both mechanical destruction and ultrasonic action lead to mechanical destruction of conglomerates of particles, formation and growth of cracks within a single element of microstructure, rupture of atomic bonds with the formation of a new surface within the lattice scale and, consequently, to appearance of piezoelectric fields, motion and multiplication of dislocations in the stress field created by external action (influence). Motion of dislocations in crystallites plays an essential role for quenching the band. The influence of pulsed magnetic field, which leads to a considerable (~double) quenching the band with $\lambda_{max} \sim$ 455 nm, according to [38], can lead, mainly, to dislocations detachment from their stoppers, i.e. to the increase of dislocations mobility and to the change in localization of the Kottrell atmosphere, tracing the motion of dislocations, but any greater changes in the material as a result of PMF are excluded. This confirms the assumption about the localization of centres, responsible for emittance of the band with $\lambda_{max} \sim$ 455 nm in the regions of dislocation clusters, where inner boundaries easely arise and in the regions adjoining to these boundaries.

The actions of SHF-radiation and ultrasonic action have also close results of intensity redistribution in the bands making up the photoluminescent band with $\lambda_{max} \sim$ 590 nm. It is indicative of their almost identical efficiency of influincing radiation centres including Mn. Both these actions are accompanied by a great number of electrical breakdowns in spacings between neighboring particles, which are caused by local alternating strain, development of self-spread plasma-chemical reactions in incomplete channels of breakdowns and in upper parts of spreading microcracks, by microplastic instability manifestation and by local warming up. Meanwhile, plastic strain plays a dominant role, provided that there is a concentration drop of Mn ions, located in zinc sublattice, in severely perturbed and disordered lattice sites, relative to $Mn^{2+}$ close to dislocations and isolated defects, i.e. in case of the change of the ratio of the bands with $\lambda_{max} =$ 557 and 578 nm. It follows from the peak drop of the band with $\lambda_{max}$=557 nm as regard to the band with $\lambda_{max}$=578 nm under mechanical destruction. When influencing the ratio of the bands with $\lambda_{max} =$ 600 and 578 nm, the role of plastic strain turns to be minimum. The maximum relative drop of $Mn^{2+}$ concentration in octahedral

interstices (bands with $\lambda_{max}$ = 600 nm) is realized by increasing mobility of dislocations, i.e. at PMF treatment. Evidently, PMF leads to the growth of the band with $\lambda_{max}$ = 578 nm, i.e. to the increase of $Mn^{2+}$ quantity in the areas close to dislocations or point defects, rather than to the intensity drop of the band with $\lambda_{max}$ = 600 nm. This is also confirmed by the fact that PMF processing leads to the maximum growth of the elementary Mn bands in luminescent spectra. Let us note that radiation of Mn ions is sensibilized, i.e. the exciting light energy is mainly absorbed by the centres called sensitizers, which role in ZnS:Mn can be carried out by the defects located nearby and impurities (Cl, O etc.), and then it is transmitted to a radiating Mn ion (activator) [35]. Therefore, the intensity growth of Mn bands in excitation spectra is indicative of the efficiency growth of the resonance channels participating in excitation of $Mn^{2+}$ luminescence as regard to the efficiency of the band-to-band channel. As in the areas surrounding dislocations there are, as a rule, the Kottrell atmospheres, where the concentration of sensitization centres is elevated [39], the increase in efficiency of Mn centres under PMF treatment is, evidently, related to the migration of dislocations under the influence of Coulomb force on $Mn^{2+}$.

## 6. Conclusion

Proceeding from the resuls mentioned above, it follows that diminishing the sizes of ZnS:Mn crystals, obtained by the SHS method, as well as more accurate separating the phases, available in the material by developing and increasing inner boundaries and the surface under the influence of external actions (mechanical destruction, ultrasonic action, SHF-radiation and pulsed magnetic field) leads to quenching in the region ~400–525 nm of its SA-luminescence. These results correlate very accurately with the model, considering peculiarities of ZnS structure formation under the growth of the electrical moment in material crystallites with increasing the surface area of their facets that are perpendicular to piezoelectric axes. In other words, when achieving a certain value of small-sized ZnS crystallites under the influence of external actions, metastable neighbourhood $V_{Zn}$ and $Zn_i$ in the centres responsible for SA-luminescence becomes unstable and leads to either their annihilation, or to their considerable moving away and locking in a new place, which prevents their migration and subsequent annihilation. In this case, annihilation of $V_{Zn}$ and $Zn_i$, evidently, proves to be the dominant process, as the possibility of locking interstitial zinc, which has high mobility in ZnS [20], seems to be of a low probability. However, a certain quantity of vacancies, which are the main suppliers of charge carriers in ZnS, according to the notions of piezoelectric properties, is necessary for neutralization of the electrical moment even in small crystallites. In support of a steady neighbourhood of $V_{Zn}$ and interstitial cation, tells a considerable quantity of $Mn_i$, responsible for the bands with $\lambda_{max}$ = 600 and 578 nm, and available in the material both directly after synthesis and after processings.

Thus, proceeding from the model, presented above and explaining the causes, leading to the development of defects responsible for SA-luminescence in the course of ZnS growth, it becomes clearer the causes of degradation of electroscintillation indicators based on ZnS, as well as the causes of complications arising at preparation of oxygen-free and *p*-type ZnS.

*References*


1. I.E. Molodetskaia, S.V. Kozitsky, D.D. Polishchuk, Features of structure formation of zinc sulfide produced by self-propagating high-temperature synthesis // *Izvestiia AN USSR. Neorganich. materialy*, **27**(6), p. 1142-1146 (1991), in Russian.
2. Yu.V. Vorobyov, V.N. Zakharchenko and S.V. Kozitsky, Electrical properties of zinc sulfide produced by self-propagating high-temperature synthesis // *Quantum Electronics*, (**4**), p. 73-79 (1995).
3. N.P. Golubeva and M.V. Fok, Luminescence of ZnS crystals with p-type conduction // *Journal of Applied Spectroscopy*, **43**(6), p. 1340-1342 (1985).
4. N.P. Golubeva and M.V. Fok, The oxygen-associated luminescence of “impurity-free” zinc // *Journal of Applied Spectroscopy*, **17**(2), p. 1025-1030 (1972).
5. N.K. Morozova, V.A. Kuznetsov, M.V. Fok, *Zinc Sulfide: Preparation and Optical Properties*. Nauka, Moscow (1987), in Russian.
6. A.K. Mc’Curdy, Phonon focusing and phonon conduction in hexagonal crystals in the boundary-scattering regime // *Phys. Rev. B*, **9**(2), p. 466-482 (1974).
7. V.V. Zubritskii, Phonon focusing in CdSe, ZnS, and ZnO crystals // *Technical Physics*, **67**(6), p. 639-643 (1997).
8. E.I. Perov, Thermodynamics and kinetics of processes of synthesis of compounds with alternative content and materials based on them // *Diss. for degree of Doctor of chemistry sci.: Code 02.00.04; RGB OD 71:05-2/36 2004, Tomsk*, (in Russian).
9. I.V. Tananaev, V.B. Fedorov, E.G. Kalashnikov, Physics-and-chemistry of energy-saturated media // *Uspekhi Khimii,* **56**(2), p. 107-120 (1987), in Russian.
10. P.M. Zorky, *Symmetry of Molecules and Crystalline Structures*, ed. M.A. Poraj-Koshits. Moscow University Publishing House, 1986 (in Russian).
11. V.L. Ginzburg, Theory of ferroelectric phenomena // *Physics-Uspekhi*, **38**(8), p. 490-525 (1949).
12. J.M. Poplavko, L.P. Pereverzev, I.P. Raevsky, *Physics of Active Dielectrics*. Rostov n/D, Publishing house of the South Federal University, 2008.

13. D.N. Shevarenkov, A.F. Shchurov, Dielectric properties of polycrystalline ZnS // *Semiconductors*, **40**(1), p. 33-35 (2006).
14. A.F. Shchurov, V.A. Perevoshchikov, T.A. Grachev, N.D. Malygin, D.N. Shevarenkov, E.M. Gavrishchuk, V.B. Ikonnikov, E.V. Yashin, Structure and mechanical properties of polycrystalline zinc sulfide // *Inorganic materials*, **40**(2), p. 96-101 (2004).
15. L.M. Kovba, V.K. Trunov, *X-ray Phase Analysis*. Moscow University Publishing House, 1976 (in Russian).
16. N.K. Morozova, I.A. Karetnikov, V.V. Blinov and E.M. Gavrishchuk, A study of luminescence centers related to copper and oxygen in ZnSe // *Semiconductors*, **35**(1), p. 24-32 (2001).
17. N.K. Morozova, D.A. Mideros, V.G. Galstyan and E.M. Gavrishchuk, Specific features of luminescence spectra of ZnS:O and ZnS:Cu(O) crystals in the context of the theory of non-intersecting bands // *Semiconductors*, **42**(9), p. 1023-1029 (2008).
18. N.K. Morozova, D.A. Mideros, E.M. Gavrishchuk and V.G. Galstyan, Role of background O and Cu impurities in the optics of ZnSe crystals in the context of the model of non-intersecting bands // *Semiconductors*, **42**(2), p. 131-136 (2008).
19. N.K. Morozova, D.A. Mideros and N.D. Danilevich, Absorption, luminescence excitation, and infrared transmittance spectra of ZnS(O)-ZnSe(O) crystals in the context of the model of non-intersecting bands // *Semiconductors*, **43**(2), p. 162-167 (2009).
20. N.K. Morozova, I.A. Karetnikov, V.G. Plotnichenko, E.M. Gavrishchuk, É.V. Yashina and V.B. Ikonnikov, Transformation of luminescence centers in CVD ZnS films subjected to a high hydrostatic pressure // *Semiconductors*, **38**(1), p. 36-41 (2004).
21. S.V. Bulyarskii and A.S. Basaev, Thermodynamics and kinetics of adsorption of atoms and molecules by carbon nanotubes // *Journal of Experimental and Theoretical Physics*, **108**(4), p. 688-698 (2009).
22. V.B. Fedoseyev, Excess free energy of solution during sedimentation of particles of a solved component // *The bulletin of the N.I. Lobachevsky Nizhniy Novgorod University*, **1**(3), p. 94 (2001), in Russian.
23. N.J. Sdobniakov, On stability conditions of small particles in the condensed phase // *The bulletin of Tver State University. Phys. Ser*. **4**(6), p. 158 (2004), in Russian.
24. B.G. Novitskiy, *Application of Acoustic Vibrations in Chemical-and-technological Processes (Processes and Devices of Chemical and Petrochemical Technology)*. Chemistry, Moscow, 1983 (in Russian).
25. Yu.K. Kovneristy, I.Yu. Lazareva and A.A. Ravayev, *Materials Absorbing Microwave Radiation*. Nauka, Moscow, 1982 (in Russian).
26. A.S. Lagutin, V.I. Ozhogin, *Pulsed Magnetic Fields in Physical Experiments*. Energoatomizdat, Moscow, 1988 (in Russian).
27. N.D. Borisenko, M.F. Bulanyi, F.F. Kodzhespirov, B.A. Polezhaev, Properties of emission centers in manganese-doped zinc sulfide // *Journal of Applied Spectroscopy*, **55**(3), p. 905-910 (1991).
28. M.F. Bulanyi, B.A. Polezhaev, T.A. Prokofiev, I.M. Chernenko, Excitation spectra and structure of luminescence centers of manganese ions in single crystals of zinc sulfide // *Journal of Applied Spectroscopy*, **67**(2), pp. 282-286 (2000).
29. W. Busse, H. Gumlish, R.O. Tornqvist, V. Tanninen, Angular overlap model for the Jahn–Teller coupling constants in the orbital triplet states of $d^5$ ions: Case of $Mn^{2+}$ in ZnS and ZnSe // *Phys. Status Solidi* (*a*), **76**, p. 553 (1983).
30. W. Busse, H.-E. Gumlich, A. Geoffroy, R. Parrot, Spectral distribution and decay times of the luminescence of $Mn^{2+}$ in different lattice sites in ZnS // *Phys. Status Solidi* (*b*), **93**, p. 591-596 (1979).
31. T.V. Butkhuzi, A.N. Georgobiani, Ye. Zada-Uly, B.T. El'tazarov, T.G. Khulordava, Luminescence in single-crystal layers of zinc oxide with n- and p-type conductivity // *Trudy FIAN*. **182**, p. 140-187 (1987), in Russian.
32. V.F. Tunitskaya, T.F. Filina, E.I. Panasiuk, Z.P. Ilyukhina, The temperature properties of the individual blue bands of self-activated zinc sulfide and the nature of corresponding radiative centers // *Journal of Applied Spectroscopy*, **14**(2), p. 182-186 (1971).
33. A.N. Georgobiani, M.K. Sheinkman, *Physics of $A^{II}B^{VI}$ Compounds*. Nauka, Moscow, 1986 (in Russian).
34. I.V. Ostrovsky, *Acoustoluminescence and Defects in Crystals*. Vyshcha shkola, Kiev, 1993 (in Russian).
35. V.F. Agekian, Intracenter transitions of iron-group ions in II–VI semiconductor matrices // *Physics of the Solid State*, **44**(11), p. 2013-2030 (2002).
36. V.A. Goriunov, E.J. Zinchenko, V.S. Mordiuk, Computer simulation of influence of the density and nature of the dislocation distribution on the intensity of luminophor luminescence // *Izvestiia vysshikh uchebnykh zavedenii. Povolzhskii region. Tekhnich. nauki.* **1**(13), p. 73 (2010), in Russian.
37. A.I. Olemskoi, I.A. Sklyar, Evolution of the defect structure of a solid during plastic deformation // *Physics-Uspekhi*, **35**(6), p. 455-480 (1992).
38. Yu.I. Golovin, Magnetoplastic effects in solids // *Physics of the Solid State*, **46**(5), p. 789-824 (2004).
39. S.A. Omel'chenko, M.F. Bulanyi and O.V. Khmelenko, Effect of the electric fields of immobile dislocations on photoluminescence and EPR in deformed ZnS crystals // *Physics of the Solid State*, **45**(9), p. 1688-1693 (2003).